Weather radar online Sun-monitoring in presence of leverage outliers: five or three parameter model inversion?

Patricia Altube[1,2], Joan Bech[2], Oriol Argemí[1], Tomeu Rigo[1], and Nicolau Pineda[1]

[1]*Servei Meteorològic de Catalunya, Berlin 38-48, 08029 Barcelona, Spain*
[2]*Dpt. Astronomia i Meteorologia, Universitat de Barcelona, Martí i Franquès 1, 08028 Barcelona, Spain*

(Dated: 18 July 2014)

1. Introduction

Continuous evaluation of the weather radar system status is an important source of dynamic information on data quality control and characterization. In particular, the procedure for online and simultaneous Sun-monitoring of weather radar antenna alignment and receiver chain calibration presented and developed in a series of works by Holleman and Beekhuis (2004), Huuskonen and Holleman (2007) and Holleman et al. (2010) is currently operational in several European Meteorological Services. The method consists on fitting, to daily detected solar signatures, a theoretical model for the power of the solar signal observed by the scanning radar.

Recently, the method has been adapted to the short to mid range data (50-150 km) available from the weather radar network (XRAD) of the Meteorological Service of Catalonia (SMC). Also, the theoretical model for solar interference observations has been reviewed providing a means to estimate the effective scanning beamwidth directly from radar technical and scanning settings. In this work, the observational data collected by the different XRAD radar systems is used as base for an analysis of the stability and accuracy of a three-parameter model fit in comparison to a full five-parameter retrieval.

2. Methodology

Following Holleman and Beekhuis (2004), online application of the Sun interference method requires automatic detection of solar artifacts in polar reflectivity data, which constitute input observations for a 2-dimensional Gaussian model. The theoretical model describes the detected power dependent on the relative displacement between the antenna axis and the Sun disk centre. Inversion of the model yields an estimation of the antenna pointing bias and of the solar power at the Top Of the Atmosphere (TOA) as detected by the radar. Comparison of this estimation with reference solar flux data from Dominion Radio Astrophysical Observatory (DRAO) allows the assessment of the receiver calibration status

2.1. Sun interference detection and characterization

Originally, the Sun interference detection algorithm was designed for application to radar scans reaching long range scopes. A radial with a reflectivity value in all or most of its bins at long ranges, where the presence of precipitation and ground echoes is minimal, is a main candidate as a solar interference (Huuskonen and Holleman, 2007).

Given the range characteristics of the XRAD systems (reaching a maximum of 130-150 km in their volumetric scans), setting an appropriate minimum beam range-height criterion implies to exclude scanned elevations up to 3° from the analysis. Hence, the detection and characterization procedure has been modified and adapted to allow for application of the monitoring method to solar artifacts found at all scan elevations even when only data at relatively short ranges is available. A flow-chart in Figure 1 schematically depicts the adapted process. Note that for a first identification only a short 50 km range threshold is set so that the areas close to the radar site most affected by ground clutter are skipped. In the process of solar signal power characterization the range threshold is slightly moved away to 80 km and a statistical deviation maximum threshold of 2dB (set in an *ad-hoc* complementary analysis) for the median power of the interference radial is established. This is useful in limiting the error of the interference power and in discarding interferences strongly affected by ground clutter or precipitation echoes.

 paltube@meteo.cat

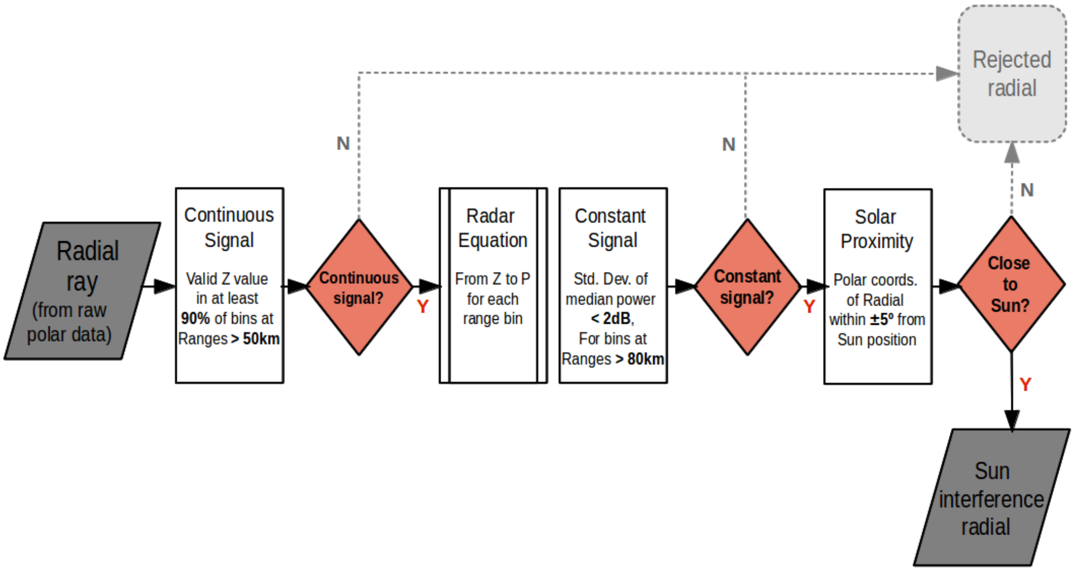

Figure 1: Flow chart of the Sun interference identification algorithm. Main quantitative criteria are highlighted in boldface and define a disjunctive step in which either the radial is discarded or kept as potential Sun interference to continue towards next processing steps.

2.2. Sun interference model

The power of the Sun signal as detected by the radar is modeled considering the emission-reception scheme of the pulsed system while the antenna is in (azimuthal) motion. For a single reception sample, the fraction of solar power detected may be quantified by the convolution between the solar power pattern -a uniform disk of Δ_S diameter- and the antenna gain pattern -symmetric Gaussian with Δ_B the 3-dB beamwidth-(Holleman et al., 2010). In turn, the detected power is calculated by the radar processor as the average of the power values measured in the collection of consecutive samples taken while scanning a radial. Summation over the samples may be approximated by an integral when the sampling interval is small compared to the total width of the radial, Δ_R. The model function resulting from the latter integral closely resembles a Gaussian for values of approximately $\Delta_R/\Delta_B \leq 1.5$ (Blahak, 2008). The typical width of the Gaussian or the scanning effective beamwidth in reception ($\Delta_{B,\text{eff}}$) may be estimated from the solution of the following transcendental equation (in analogy to Doviak and Zrnic (2006, Ch. 7.8)):

$$\left\{ \text{erf}\left[\frac{\sqrt{4\ln 2}}{\Delta_B}\left(x+\frac{\Delta_R}{2}\right)\right] - \text{erf}\left[\frac{\sqrt{4\ln 2}}{\Delta_B}\left(x-\frac{\Delta_R}{2}\right)\right] - \frac{2}{e}\,\text{erf}\left(\sqrt{\ln 2}\,\frac{\Delta_R}{\Delta_B}\right)\right\}_{x=\pm x^\star} = 0\,, \tag{2.1}$$

being $x^\star$ the positive root of the equation and $\Delta_{B,\text{eff}} = 2\sqrt{\ln 2}\,x^\star$.

Under these conditions, the resulting model is, as proposed by Holleman et al. (2010):

$$p_{\text{det}} = l_{\text{atm}}\, l_{\text{scan}}\, p_{\text{TOA}}\, \exp\left\{-4\ln 2\left[\frac{(x-x_0)^2}{\Delta^2_{B,\text{eff}}} + \frac{(y-y_0)^2}{\Delta^2_B}\right]\right\}. \tag{2.2}$$

with

$$l_{\text{scan}} = \frac{1}{\ln 2}\,\frac{\Delta^2_B}{\Delta^2_S}\left[1-\exp\left(-\ln 2\,\frac{\Delta^2_S}{\Delta^2_B}\right)\right]\sqrt{\frac{\pi}{4\ln 2}}\,\frac{\Delta_B}{\Delta_R}\,\text{erf}\left(\sqrt{\ln 2}\,\frac{\Delta_R}{\Delta_B}\right). \tag{2.3}$$

where $(x,\,y)$ coordinates denote the relative distances (in azimuth and elevation, respectively) between the central position of the antenna in the radial and the Sun disk centre; p_{TOA} is the solar power at the TOA as seen by the radar system and l_{atm} is a factor accounting for the solar power attenuation in its path across the atmosphere (Huuskonen and Holleman, 2007).

The model Equation (2.2) applied to the input observations (i.e. the powers of the detected solar interferences, each corrected for l_{atm}) constitutes a nonlinear inverse problem. Linearization and direct inversion by means of a Linear Least Squares (LLS) procedure is applied (Holleman and Beekhuis, 2004) to retrieve the target model parameters. These are the solar power p_{TOA} in dBm, the (x_0, y_0) systematic antenna pointing biases in azimuth and elevation (3 parameter model inversion; 3P model) and, optionally, also the effective angular beamwidths in azimuth $\Delta_{B,\text{eff}}$ and elevation Δ_B (full 5 parameter model inversion; 5P model), whose values are known or can be estimated from Equation (2.1).

2.3. Outliers

The sensitivity of LLS estimates to the presence of model outliers is exemplified in the model fit of Puig d'Arques (PDA) radar displayed in Figure 2. Notice the outlying observation on the upper-left corner of the plot that acts as main driver in the fit outcome. PDA commonly presents these strong outliers, likely related to emission from R-LAN systems located close to the radar site. Problematic observations may also be present due to inaccurate estimation of the detected power (e.g. presence of precipitation or attenuation) or to an inaccurate positioning of the Sun relative to the interference, for instance.

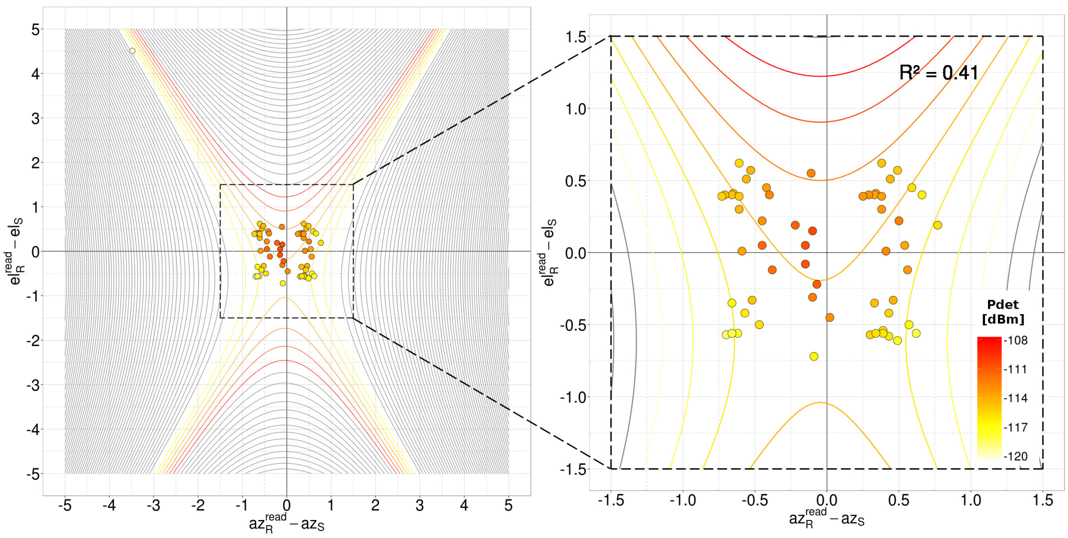

Figure 2: Performance of the daily (5P model) fit to interference observations before outlier removal for PDA radar (10 June 2013): regular model fit using all identified interferences (left panel) and zoom into the framed region (right panel). Observations are scattered by the relative position between the interference radial and the Sun.

A simple, non-iterative procedure for the removal of biased observations prior to inversion is proposed. The criterion is based on the assumption that, if the pointing bias is small (below $\approx 0.1°$), the collection of solar powers at the TOA, as derived from Equation (2.2) for each of the Sun interference observations, should display a normal distribution with an expected value ca. the actual P_{TOA}. Hence, the median and the standard deviation estimator are computed for the target Sun interference sample and observations whose individual solar power at the TOA is not within the 2-σ interval around the median, are rejected as outliers (Sprent and Smeeton, 2007).

Figure 3 shows the resulting model fit for the aforementioned PDA example after outlier removal criterion application. In addition, the use of robust estimators has proven effective in the identification of very influential outliers (leverage outliers) even if a significant antenna pointing bias is present.

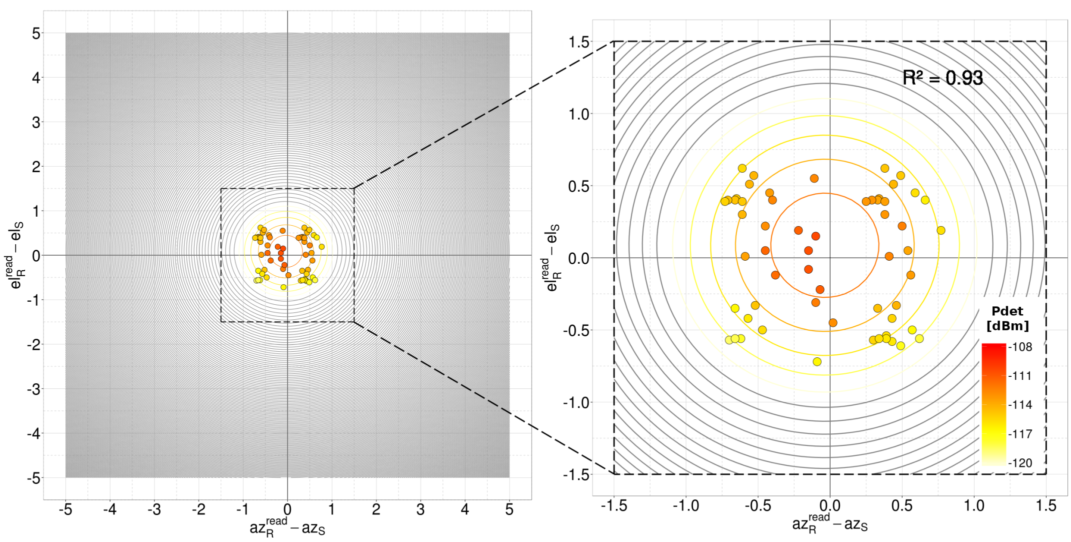

Figure 3: As Figure 2 but for interference observations after outlier removal.

3. Application to XRAD

The Sun monitoring algorithm has been implemented for three C-band, single polarization operative Doppler weather radars of the SMC network (the XRAD): Creu del Vent (CDV), La Miranda (LMI) and Puig d'Arques (PDA). Application of the method to a year (2013) of daily data and comparison between the 5P and the 3P model inversion approaches has revealed a distinct performance for each radar case.

The 5P-model inversion turned out to be working best for PDA radar; although no relevant difference in the stability of the fit results was appreciated whether the 5P or the 3P model fit was applied, the 5P model inversion yielded higher R-squared values of the fit. By contrast, for LMI, the convergence, the stability and uncertainty of the model parameter estimates (mainly the pointing bias in azimuthal direction) was significantly improved when using the 3P fit. A better performance of the 3P model inversion was also registered for CDV radar during the first half of the year.

An inspection of which conditions may be involved in the observed performance of the method pointed to the number of observations collected and to their spatial distribution prior to the fit. Hence, a sensitivity analysis was carried on with the aim of quantifying the particular influence of these aspects. In the analysis, the relative positions of actual observations with respect to the Sun were used as input.

3.1. Sensitivity analysis

Solar observations collected by each of the radars during selected time periods conform three distinct distributions as a function of the relative position between the interference radial and the Sun. The distributions are plotted in Figure 4 and their assigned names make reference to the shape displayed. The *Butterfly* (BU) distribution corresponds to observations collected by CDV radar from January to May 2013, coinciding with a period of emitter malfunction; the *Circular* (CI) distribution, in turn, corresponds to observations collected by LMI radar from July to November 2013 and its shape relates to a low sensitivity of the receiving system that allows detection of solar signatures only for antenna positions close to the Sun; finally, the *Elliptical* (EL) distribution collects observations by PDA radar from January to April 2013 and is expected to be optimal for the retrieval of the target model parameters.

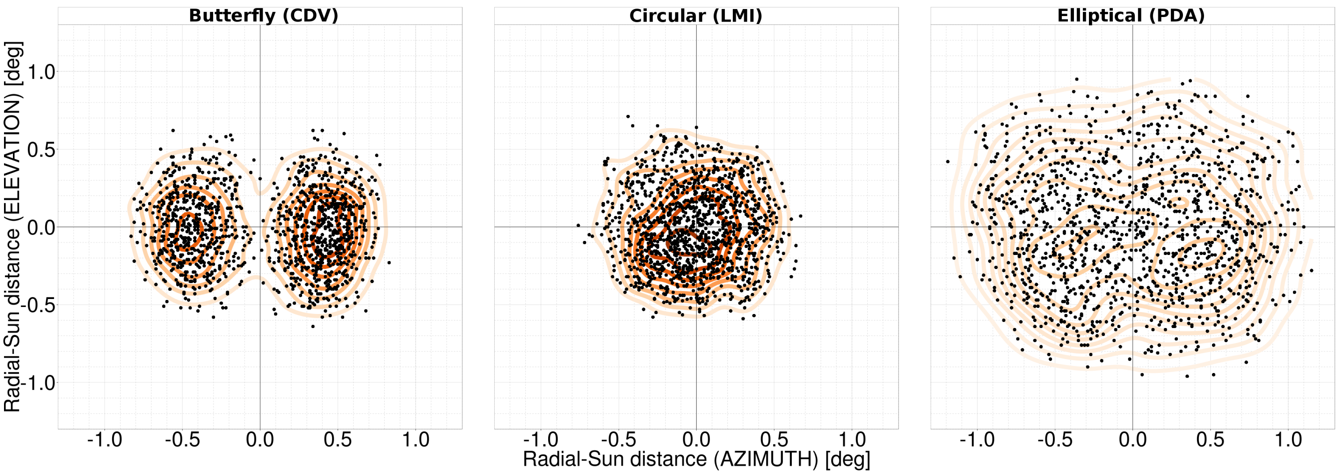

Figure 4: Target distributions of observations compared in the model performance analysis. Equal point-density lines are also displayed, with darker colours indicating a higher density.

The sensitivity analysis consists on randomly selecting a certain number of observations (N) from each of the target distributions. Then, for each of these N observations, the detected solar power is modelled through Equation 2.2 with addition of multiplicative random noise (of 0.5 dB standard deviation). After including artificial systematic antenna pointing biases ($+0.2°$ in azimuth and $-0.3°$ in elevation) and detected power offset (+1 dB), model parameters are estimated in both 3P and 5P model fits. The number of observations N is varied from 6 to 100 and the procedure described above is repeated 500 times in each case.

Figure 5 shows the resulting statistics of method accuracy, derived from the comparison between fit parameter estimates and their nominal values, as a function of the number observations and for the three different distributions. Results indicate that for large number of observations ($N \gtrsim 30$) the accuracy in the antenna pointing bias estimation is high, with a maximum error within $0.01°$ and $0.03°$, and independent of the inversion approach used. When the number of observations is low ($N \lesssim 20$) pointing bias estimates become unstable and differences between the distributions and between inversion approaches become significant. In such case, the 3P model inversion limits the maximum accuracy error, which is most notable for the CI distribution in azimuth ($\approx 0.15°$) an for the BU distribution in elevation ($\approx 0.12°$). For the 5P model inversion, corresponding maximum accuracy errors go beyond $0.20°$. On the other hand, results show how the choice of either the 3P-model or the 5P-model fit has an impact on the accuracy of the reception power calibration; the maximum error for the 3P-model case goes from 0.1 dB for large N to ca. 0.5 dB for lower N whereas, for the 5P-model, corresponding errors go from 0.2 dB to more than 1 dB and show slight differences depending on the distribution considered. This performance may be due to the probability of finding observations very close to the Sun being generally lower than at medium relative distances (particularly in azimuthal direction, see Figure 4) together with the additional adjustment of beamwidths in the 5P-model inversion. This might also explain the trend to overestimation of the solar power when N decreases and the relatively higher accuracy of the power estimates for the CI distribution when N is large, which indeed seems related to a higher inaccuracy in the estimation of beamwidths, particularly in azimuthal direction (not shown).

Maximum accuracy errors in the estimation of the effective beamwidths have been likewise found to be ca. $0.1°$ for $N \gtrsim 30$ ($0.2°$ in the case of CI distribution) and around $0.5°$ for $N \lesssim 20$ (although may go beyond $1°$ for CI and BU distributions).

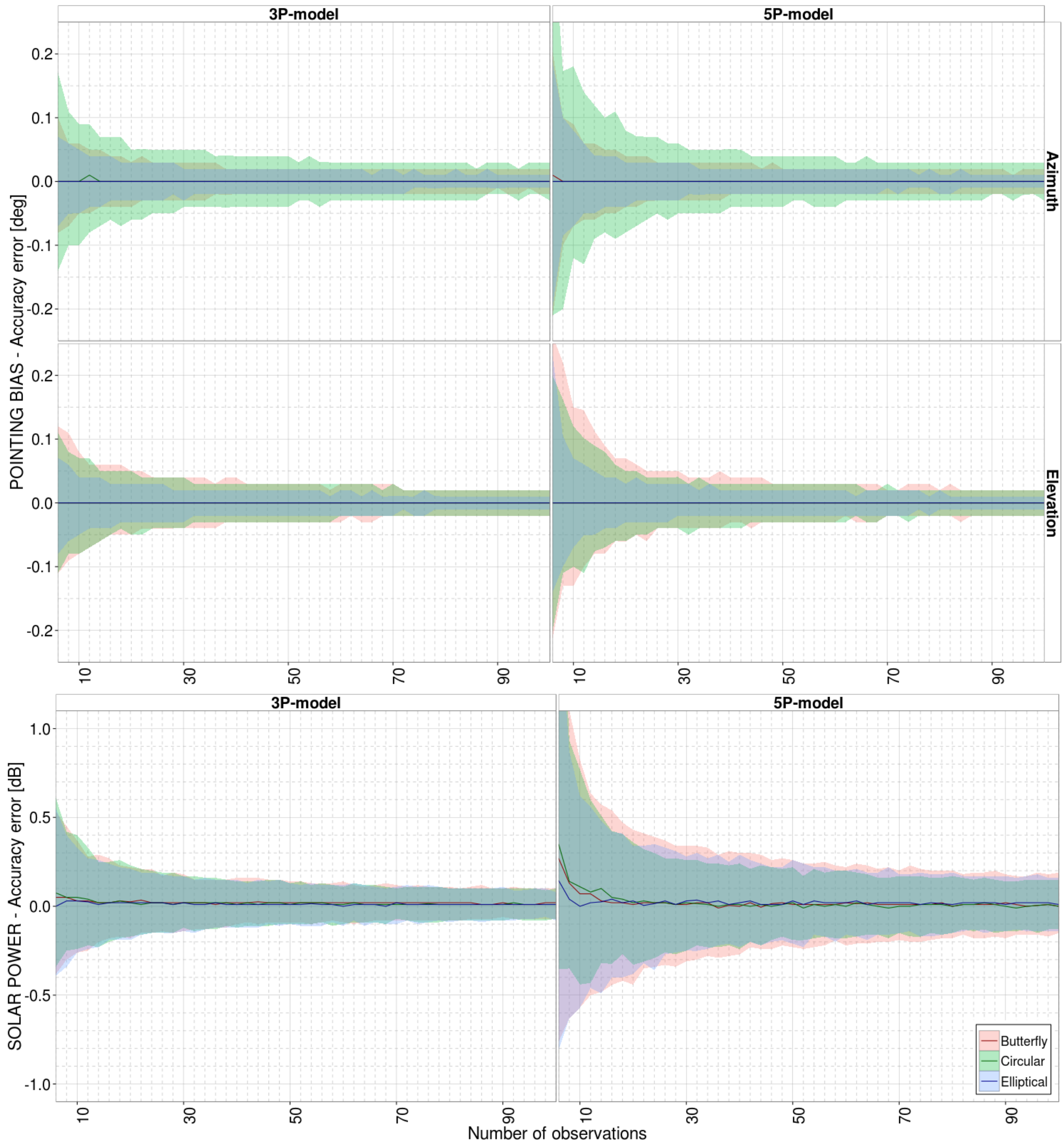

Figure 5: Accuracy of antenna pointing bias and solar power at the TOA parameter estimates in the Sun-monitoring method as derived from the performance analysis. Median accuracy error (solid lines) and its P05-P95 inter-percentile range (enclosed in shaded areas) are displayed as a function of the number of observations considered and for the three different target distributions (circular, elliptical and butterfly-shaped). 3-parameter (left panels) and 5-parameter (right panels) model inversions are shown in comparison.

4. Summary and conclusions

The online Sun detection method for combined monitoring of weather radar antenna pointing biases and receiver calibration is applied to the weather radar network of the SMC. The algorithm for the detection and characterization of Sun interferences is adapted to allow for application to data at short to mid ranges. A revision of the physical model provides a means for analytically estimating the effective beamwidth in reception of a scanning antenna. Before model inversion, application of a non-iterative method based on robust statistical estimators proves effective for the removal of leverage model outliers.

A method performance study reveals that the accuracy and stability of the antenna pointing bias and solar power estimates are strongly influenced by the number of observations collected. When the number of observations decreases below ca. 20, accuracy in the estimates decreases and their values become increasingly unstable. In such case, application of the 3P-model inversion may be advisable since it yields more accurate and stable parameter values of limited uncertainty. The influence of the shape of the distribution conformed by the observations is most noticeable for small data-sets and particularly affects the median accuracy of the solar power estimates. As a significative case, observations collected by radar systems with low sensitivity relative to the solar signal (CI distribution), which tend to lack data in the direction of the antenna scanning motion, do not carry information enough for the method to yield as accurate and precise estimates of the pointing bias and beamwidth in that direction.

For a number of observations above ca. 30, accuracy values remain invariant and the 3P-model and 5P-model inversion approaches perform similarly. While the 5P-model parameter estimates tend to present higher accuracy error in the solar power estimation, the 3P-model parameter values may be subject to the effect of an inaccurate choice of the fixed effective beamwidths (which is not considered in the performance analysis). The former is likely related to the coupling with the inherent inaccuracy in the adjustment of the beamwidths and to the data-point density distribution. However, beamwidth estimates from the 5P model fit may give additional information on the pointing stability of the antenna system as stated by Huuskonen et al. (2010).

In all situations results indicate that the median of several consecutive estimates is a very accurate indicator of the actual antenna pointing bias (maximum median error below $0.01°$, matching the mechanical resolution) and solar power signal (maximum median error below 0.5 dB, the sensitivity attributed in the radar processor).

Acknowledgments

Thanks are due to the DRAO (National Research Council Canada) for providing open access reference solar power measurements. The present research was carried out in the framework of the Industrial Doctorate Projects partly funded by the Autonomous Government of the Generalitat de Catalunya.

References

U. Blahak, "An approximation to the effective beam weighting function for scanning meteorological radars with an axisymmetric antenna pattern," *J. Atmos. Oceanic Technol.*, vol. 25, pp. 1182–1196, 2008.

R. J. Doviak and D. S. Zrnic, *Doppler radar and weather observations*, 2nd ed. Dover Publications, 2006.

I. Holleman and H. Beekhuis, "Weather radar monitoring using the Sun," Royal Netherlands Meteorological Institute, KNMI Tech. Rep. TR-272, 2004.

I. Holleman, A. Huuskonen, M. Kurri, and H. Beekhuis, "Operational monitoring of weather radar receiving chain using the Sun," *J. Atmos. Oceanic Technol.*, vol. 27, pp. 159–166, 2010.

A. Huuskonen and I. Holleman, "Determining weather radar antenna pointing using signals detected from the Sun at low antenna elevations," *J. Atmos. Oceanic Technol.*, vol. 24, no. 3, pp. 476–483, 2007.

A. Huuskonen, H. Hohti, T. Kuitunen, and M. Kurri, "The use of the solar monitoring data to assess the quality and the stability of weather radar antenna systems," in *TECO-2010, WMO Technical Conference on Meteorological and Environmental Instruments and Methods of Observation*, Helsinki, Finland, 2010, p. 6.

P. Sprent and N. C. Smeeton, *Applied nonparametric statistical methods*, 4th ed. Chapman and Hall/CRC, 2007.